

## Prediction of dendritic micro-heterogeneity of cast steel: review of models and computer-aided analysis of problems (Part 2. Analysis of influence of steel components)

V. M. Golod<sup>1</sup>, K. I. Emelyanov<sup>1</sup>, I. G. Orlova<sup>1</sup>

<sup>1</sup> Saint-Petersburg State Polytechnic University  
(St. Petersburg, Russia)

E-mail: cheshire@front.ru

© Golod V. M., Emelyanov K. I., Orlova I. G., 2013

*The article (the second part of the overall review) reviews the publications on dependence of secondary dendrite arm spacing microstructure of industrial iron-based alloys from their chemical composition. It is noted that quantification of this effect obtained by experiments and presented by statistical models, are characterized by significant differences in mathematical form, as well as the sign and magnitude of the regression coefficients which evaluate the contribution of different components of steel. By graphical comparison of published empirical models, it is established that the dependence of the dendrite arm spacing of carbon and low alloy steels from carbon content has the contradictory character, that does not allow its unambiguous quantitative evaluation and detection the determining factors.*

*Analysis of this situation shows that improving the quality of statistical models (the exception of insignificant effects caused by certain components, elimination the correlation distortion, etc.) and for ensuring of their adequacy it is reasonably to unify the description of the experimental data on the basis of a polynomial form of the concentration term of the regression equation, obtained by means of orthogonal experimental design.*

*The role of physical-chemical and thermal factors in the development of coalescence of secondary arms is quantified by numerical calculation of the dendritic structure produced by computer simulation of non-equilibrium solidification of steel slabs (250 mm thickness) with calculation of the changes in the composition of the liquid phase and the evolution of interdendritic spacing. It is established that reduction of the secondary dendrite spacing in carbon and low alloy steels with growth of carbon, silicon, manganese, chromium, and nickel content, as well as the increase in the proportion of austenite during solidification, is caused by suppression of diffusion transport of components during coalescence of dendritic branches. A quantitative evaluation of the intensity of the process, defined by the concentrations of components and a number of thermodynamic (a slope of the liquidus, the distribution coefficient) and kinetic (diffusion coefficient in the melt, the Gibbs-Thomson coefficient) parameters decreases in the following sequence: C, Si, Mn, Ni, Cr.*

**Key words:** carbon and low-alloy steel, dendritic structure, dendrite arm spacing, empirical power-type models, computer modeling, non-equilibrium crystallization.

The main object of this review and corresponding analysis, as in [36], are secondary dendritic arm spacing  $\lambda_2$  and in particular — their effect on the values of different components of industrial multi-component alloys (carbon and low-alloy steels), revealing their separate and/or joint appearance as well as factors of different nature that determine these effects.

**Review of investigations of the effect of steel composition on the values of secondary dendritic arm spacing.** The collection of mathematical models (presented in the table 1) describes the effect of steel components on the final values of dendritic arm spacing and allows to compare the structure of developed statistical models as well as the input of separate components reflected in these models. Different features of presented formulas, obtained via the remedies of statistical simulation, and their complicated structure, chosen by the research team, attract attention at first. It is evidently that this structure is oriented only on suitable approximation of experimental data and does not suggest any physical-chemical interpretation and generalization.

The data presented in the table 1 [36] testify that the most part of the works with investigation of steels with different composition noted variation of dendritic structure depending on content of several components (first of all of carbon). However, comparison of the mathematical models presented in the table 1 displays that the effect of carbon content on  $\lambda_2$  value (defined by different researchers) can be characterized by complicated features and does not agree even by the sign of the revealed effect (see also table 1).

The work [1] needs especial attention; it describes laboratorial investigation of dendritic structure in the conditions of direct solidification of a series of low-alloy steels (containing 0.14–0.88% C at 0.46% Si and 0.65% Mn). These steels are quite different regarding the value of the temperature interval of solidification  $\Delta t_{LS}$  (36–99 K). Investigation of the structure in more than 60 (!) points of each specimen allows to establish that varying of cooling rate in the wide range (3–200 K/min) causes practically the same variations of  $\lambda_2$  value (from 60 to 500  $\mu\text{m}$ ) for different steels (see curve 3 on the fig. 1). The regression equations such as  $\lambda_2 = K_1 R^{-n}$  stipulate the values of  $K_1$  and  $n$  parameters in rather narrow range for separate alloys with different carbon content.

**Table 1. Statistical models of the effect of steel components on the values of secondary dendritic arm spacing  $\lambda_2$**

No	Formula for calculation ( $\lambda_2$ , $\mu\text{m}$ ; $R$ , K/s; $\tau_{LS}$ , s; $G_L$ , K/cm; $V_L$ , cm/s; $X_i$ : C, Si, Mn, ..., mass.%)	Conditions of use ( $X_i$ , %)	Year of publication	Reference
1	$\lambda_2 = 146R^{-0.386}$	$0.14 \leq C \leq 0.88$	1968	[1]
2	$\lambda_2 = 79C^{-0.187}\tau_{LS}^{0.38}$	$0.11 \leq C \leq 1.01$	1977	[14]
3	$\lambda_2 = A_1R^{-n}$ ; $A_1 = 148$ ; $n = 0.38$	$0 \leq C \leq 0.53$	1996	[15]
4	$\lambda_2 = A_2\tau_{LS}^d$ ; $A_2 = 21.52764 - 9.4C$ ; $d = 0.4 + 0.08C$	$0.53 \leq C \leq 1.5$		
5	$\lambda_2 = \tau_{LS}^{1/3}(70C + 50\text{Si} - 0.178\text{Mn} - 430\text{Al} + 0.755\text{Ni} + 3.42\text{Cr})$	$0.18 \leq C \leq 1.48$	1998	[9]
6	$\lambda_2 = 18.61\tau_{LS}^{0.36}\exp(1.49C)$ ; $\lambda_2 = 64.8R^{-0.36}\exp(2.12C)$ ; $\lambda_2 = 6275G_L^{-0.53}\exp(2.38C)$ ; $\lambda_2 = V_L^{-0.61}\exp(1.77C)$	$0.14 \leq C \leq 0.56$	1999	[11]
7	$\lambda_2 = (169.1 - 720.9C)R^{-0.4935}$	$0 \leq C \leq 0.15$	2001	[17]
8	$\lambda_2 = 143.9R^{-0.3616}C^{(0.5501 - 1.996C)}$	$C > 0.15$		
9	$\lambda_2 = 123R^{-0.33}\exp(A)$ ; $A = -0.281C + 0.175\text{Mn} - 0.063\text{Cr} - 0.136\text{Mo} - 0.091\text{Ni}$	—	2006	[16]
10	$\lambda_2 = (166.38 - 567.07C - 85.39C^2)R^{-0.49}$	$0 < C < 0.15$	2009	[38]
11	$\lambda_2 = (671.31C^2 - 627.8C + 232.23)R^{-0.36}C^{(0.55 - 2C)}$	$0.15 \leq C \leq 0.53$		
12	$\lambda_2 = (27.93 - 11.19C)\tau_{LS}^{(0.4 + 0.08C)}$	$C > 0.53$		
13	$\lambda_2 = (-40.02R^{-0.4} + 0.78R^{-1.11}C + 86.74R^{-0.099}\text{Si} - 38.72R^{-0.15}\text{Mn} + 1193.95R^{-0.28}\text{Al} + 1276.71R^{-0.23}\text{Cr} - 18.02R^{-0.17}\text{Ni} - 2383.63R^{-0.2}\text{Nb})\tau_{LS}^{1/3}$	$0.05 \leq C \leq 0.3$	2010	[20]
14	$\lambda_2 = 200R^{-0.33}\exp(A^{0.4})$ ; $A = -0.6844C - 0.0069\text{Si} - 0.0674\text{Mn} - 0.1412\text{Cr} - 0.0057\text{Mo} - 0.1259\text{Ni} + 0.14788C^2 + 0.00387\text{Cr}^2 + 0.00101\text{Ni}^2 - 0.10295\text{Cr}C + 0.00456\text{CrNi}$	—		
15	$\lambda_2 = 16.3(1 - 0.63\text{Si} - 0.26\text{Mn} - 0.06\text{Cr} - 0.09\text{Ni} + 0.18\text{SiMn} + 0.06\text{MnCr} + 0.02\text{MnNi})\tau_{LS}^{0.45}$	$C = 0.09$ ; $\text{Si} = 0.4$ ; $\text{Mn} = 1.2$ ; $\text{Ni} = 2.1$ ; $\text{Cr} = 1.1$	2012	[42]
16	$\lambda_2 = 18.39(1 - 0.73C)\tau_{LS}^{0.329}$	$0.01 \leq C \leq 0.07$ ; $\text{Si} = 0.3$ ; $\text{Mn} = 1$	2013	*
17	$\lambda_2 = 45.36(1 - 0.68\text{Si} - 0.49\text{Mn} - 0.26\text{Cr} - 0.68\text{Ni})\tau_{LS}^{0.33}$	$C = 0.06$ ; $X_i = 1$		
18	$\lambda_2 = 21.7(1 - 0.47\text{Si} - 0.15\text{Mn} - 0.042\text{Cr} - 0.072\text{Ni})\tau_{LS}^{0.33}$	$C = 0.6$ ; $X_i = 1$		
19	$\lambda_2 = 49.58(1 - 0.97C - 0.74\text{Si} - 0.58\text{Mn} - 0.45\text{Cr} - 0.51\text{Ni})\tau_{LS}^{0.325}$	$0.06 \leq C \leq 0.6$ ; $X_i = 1$		

Remark: \*) this work.

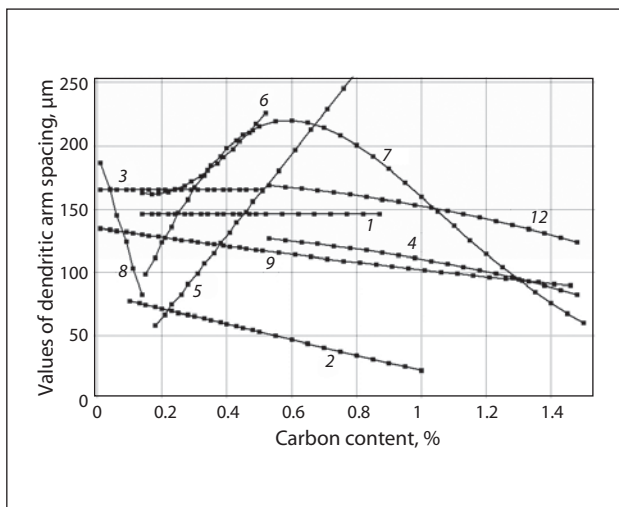


**Fig. 1. Relationship between secondary dendritic arm spacing  $\lambda_2$  and carbon content according to different models (1–12) at local time of solidification  $\tau_{LS} = 100$  s or cooling rate  $R = 0.5$  K/s. Numeration of the curves 1–12 corresponds table. 1**

On the contrary, increase of  $\lambda_2$  (curve 6 on the fig. 1), revealed during investigation of steel slabs with carbon content 0.14–0.56% (at 0.24–0.52% Si and 0.72–1.71% Mn), is explained by varying  $\Delta t_{LS}$  in the range 40–82 K [11].

As soon as the presented formulas are obtained using statistical analysis of experimental data, therefore regression coefficients in these formulas should be evaluated taking into account their relation with the confidence interval (not presented in the a.m. publications), as well as with revealing possible correlation between content of different components. The authors don't have such data, so in the case of different and complicated mathematical form of regression equations it is possible to estimate the contribution of different components only qualitatively. In particular, graphical comparison of  $\lambda_2$  (C) relationships on the fig. 1 shows that at present time there are not any reliable experimental grounds for distinct conclusions about the features of carbon effect on dispersity of dendritic structure.

**Table 2. Input of different steel components in diffusion dendrite coalescence**

Phase	Parameters	Components of alloy $X_i$					$\sum_k \frac{p_i(1-k_i)C_i^L}{D_i^L}$
		C	Si	Mn	Cr	Ni	
	$D_i^L, 10^{-9} \text{ m}^2/\text{s}$	5.41	3.74	3.71	2.57	3.01	
$\delta\text{-Fe}$	$C_0, \%$	0.01–0.09	0.2–0.6	0.6–1.2	0.1–0.5	0.1–0.5	
	$p, \text{K}/\%$	80–85	14–16	4–4.8	2.5–2.8	4–5	
	$k$	0.14–0.17	0.55–0.6	0.63–0.66	0.85–0.88	0.8–0.85	
	$p(1-k)C_0/D_i^L$	0.76–0.81	0.4–1.07	0.22–0.48	0.02–0.1	0.02–0.18	1.38–2.55
$\gamma\text{-Fe}$	$C_0, \%$	0.5–0.8	0.2–0.6	0.6–1.2	0.1–0.5	0.1–0.5	
	$p, \text{K}/\%$	70–80	20–22	2.5–3.5	1.6–2.8	2.8–3	
	$k$	0.33–0.35	0.5–0.58	0.66–0.7	0.75–0.8	0.88–0.95	
	$p(1-k)C_0/D_i^L$	5.17–6.19	0.48–1.6	0.14–0.38	0.01–0.08	0.01–0.08	5.85–8.3

The same features of dual effect also of other steel components are revealed in the table 1 by comparison of the formulas (5), (9), (13) and (14); sign change for such elements as Si, Mn, Ni and Cr is noted many times. These results can be hardly explained, if we shall not consider them as a consequence of mutual effect of the components for different composition of alloys, as well as appearance of the fact that some regression equations (those that are close to statistically non-significant ones) can change the sign in the range of a confidence interval, especially during essential mutual correlation of contents of the elements that is typical for statistical models [33, 35].

**Physical-chemical analysis of the effect of factors on the values of secondary dendritic arm spacing.** In order to find out the effect of steel components on the final dendritic arm spacing values, connected with the processes of diffusion coalescence [23, 24, 27] occurring during dendrite forming, quantitative analysis of the effect of different factors is required. Among these factors the following can be mentioned: not only physical-chemical, depending on  $C_i^L$  content for each  $i$ -component in the melt (distribution coefficient  $k$ , slope of liquidus surface  $p$ , melt diffusion coefficient  $D^L$  etc.), but also thermal-physical (liquidus and solidus temperatures  $t_L$  and  $t_S$ , crystallization heat  $Q$ , thermal capacity  $c$ , rate (tempo) of solid phase formation etc.). Systematic correlation between the marked factors is reflected by the generalized formula [24]:

$$\lambda_2^3 = \lambda_0^3 + \frac{\Gamma}{\varphi} \tau_{LS} \frac{1}{\sum_k \frac{p_i(1-k_i)C_i^L}{D_i^L}} \quad (6)$$

where  $\lambda_0$  — initial value of secondary dendrite arm spacing forming near the top of dendrite trunk;  $\varphi$  — coefficient depending on the accepted coalescence model [27, 39];  $\Gamma$  — Gibbs-Tomson coefficient;  $\tau_{LS}$  — local time of solid phase formation. Based on calculations of  $\lambda_0$  values and the results of corresponding experiments [24, 39 etc.], intensive coalescence is usu-

ally accompanied by reaching  $\lambda_2 \gg \lambda_0$ , ratio, therefore the effect of the components was evaluated during numerical simulation of the second component of the formula (6).

Varying the alloy composition causes change of transfer intensity for melt components, as well as varying time of crystallization  $\tau_{LS}$  depending on relationship between extracting heat of crystallization and intensity of external heat removal in casting conditions. Combined effect of these different factors in varying alloy composition becomes more complicated by the mutual effect of alloy components [24] and is able to cause  $\lambda_2$  variation with different value and sign.

Physical-chemical parameters shown in the table 2 are determined via thermodynamic simulation [24]. At similar values of  $D_i^L$  and  $\Gamma_i$  [40] for different steel components, incorporated in the formula (6) [24], the value of  $p_i$  and  $k_i$  coefficients, depending on the composition of multi-component liquid solution and structure of formed solid phase ( $\delta$ - or  $\gamma$ -Fe), is the most substantial. As concerns the effect on the value of the complex parameter  $p(1-k)C_0/D_i^L$  (see table 2), carbon is a decisive factor. It has maximum  $p_C$  and minimum  $k_C$  (its contribution ~30–50% at formation of  $\delta$ -phase and ~75–85% in  $\gamma$ -phase). The substitution components are located in their specific effect in the following sequence: Si (contribution 30 and 12% respectively), Mn (14 and 3%), Ni (5 and 1%), Cr (1.5 and 1%). Therefore, increase of carbon content and increase of the part of  $\gamma$ -phase causes decrease of the values of dendritic arm spacing owing to predicted intensification of the process of diffusion coalescence; it quite agrees with the features of the most curves (4, 8, 9 and 12) on final fig. 1 and with the data of table 1.

During comprehensive estimation of the effect of steel components in correspondence with (6) formula it is necessary to take into account that variation of content of the components is accompanied with substantial change of thermal-physical parameters ( $c$ ,  $L$ ) and temperature interval of solidification  $\Delta t_{LS}$ , having direct effect on  $\tau_{LS}$ .

**Table 3. Physical-chemical and thermal-physical parameters of forming final dendritic structure for non-peritectic alloys with different carbon content (0.01 < C, % < 0.07)**

Parameters of alloys	Carbon content C <sub>0</sub> , mass. %				
	0.01	0.02	0.04	0.06	0.07
Δt <sub>LS</sub> , K	10	14	22	32	37
Q, MJ/m <sup>3</sup>	1800	1821	1865	1909	1934
τ <sub>LS</sub> , s	827	830	871	912	934
R, K/s	0.01	0.02	0.03	0.04	0.04

Remarks: alloy composition: C<sub>0</sub> — 0.3% Si — 1% Mn; solidification conditions: overheating in pouring Δt = 50 K; c<sub>L</sub> = 4.8 MJ/m<sup>3</sup>·K; c<sub>S</sub> = 4.7 MJ/m<sup>3</sup>·K; α = 150 W/m<sup>2</sup>·K; physical-chemical parameters: φ = 0.048; D<sub>L</sub> = 5·10<sup>-9</sup> m<sup>2</sup>/s; Γ = 2·10<sup>-7</sup> m·K; values of τ<sub>LS</sub> and R are presented for the axial area of a billet.

**Numerical analysis of the effect of carbon on the values of secondary dendritic arm spacing.** Calculation of forming of dendritic structure has been made via numerical simulation of the conditions of solidification and dendritic crystallization of a flat billet with thickness 240 mm made of multi-component alloys of different composition on the base of the model [24, 25], presented and used in the previous chapter of this review [36]. Physical-chemical and thermal-physical parameters of investigated alloys with different content of researched components are compared in the tables 3 and 4. To calculate kinetics of variation of the values of secondary dendritic arm spacing and their final values in billet cross section, the following differential equation was used:

$$\frac{d(\lambda_2^3)}{d\tau} = \frac{\Gamma}{\varphi} \frac{1}{\sum_K \frac{p_i(1-k_i)C_i^L}{D_i^L}} \quad (7)$$

Its solution took into account variation of local composition of liquid phase C<sub>i</sub><sup>L</sup> in the conditions of non-equilibrium crystallization at restricted diffusion in solid phase [24] using equation (5) [36], as well as relationship between parameters D<sub>i</sub><sup>L</sup>, k<sub>i</sub> and p<sub>i</sub> during crystallization (from one side) and temperature (from other side). The value of φ parameter corresponds to the main coalescence model [27, 39], describing radial variation of branches of different diameter. The question about the input of different coalescence mechanisms and, respectively, about determination of the efficient value of φ parameter will be considered in the final part of this review. Calculated relationships presented in the table 3 and on the fig. 2 display that variation of carbon content in the range 0.01–0.07% slightly (by 12%) reflects on local time of solidification τ<sub>LS</sub> (fig. 2, a) and simultaneously leads to essential (by 3.3 times) increase of local cooling rate R (fig. 2, b), in connection with prominent influence of widening of solidification temperature interval Δt<sub>LS</sub>.

As a result of differences of these thermal-physical conditions in combination with variation of the values of physical-chemical parameters (see table 2) and features of diffusion processes during coalescence of dendritic structure, dimensions of dendrite arm spacing λ<sub>2</sub> (fig. 2, c, d) are varying essentially depending on carbon content, intensity of heat removal and billet cross section. Connection between dendritic structure and cooling rate R (fig. 2, d) is indirect and adds in analysis the additional factors, having no direct physical-chemical effect on the process of redistribution of the components in alloy.

Obtained calculated relationships for different alloys are described by power formulas such as λ<sub>2</sub> = K<sub>2</sub>τ<sub>LS</sub><sup>m</sup>, where exponents m are very close to 0.33 (in accordance with the formula (6)). The values of K<sub>2</sub> coefficients, corresponding to λ<sub>2</sub> value on the surface and in the center of a massive billet, are very close to

**Table 4. Thermal-physical parameters and conditions of forming dendritic structure of the alloys with different content of components**

Conditions of crystallization of alloys		Alloy composition (mass. %)				
		C <sub>0</sub>	C <sub>0</sub> + 1% Si	C <sub>0</sub> + 1% Mn	C <sub>0</sub> + 1% Cr	C <sub>0</sub> + 1% Ni
C <sub>0</sub> = 0.06% (formation of δ-phase)	Δt <sub>LS</sub> , K	22	37	26	23	25
	Q, MJ/m <sup>3</sup>	1958	1987	1951	1921	1937
	τ <sub>LS</sub> , s	537	1209	648	544	603
	D <sub>i</sub> <sup>S</sup> , 10 <sup>-9</sup> m <sup>2</sup> /s	5.2	0.037	0.019	0.021	0.014
	λ <sub>2</sub> , μm	365	152	196	272	238
C <sub>0</sub> = 0.6% (formation of γ-phase)	Δt <sub>LS</sub> , K	72	97	76	69	75
	Q, MJ/m <sup>3</sup>	2265	2317	2265	2210	2264
	τ <sub>LS</sub> , s	1210	1484	1244	1177	1230
	D <sub>i</sub> <sup>S</sup> , 10 <sup>-10</sup> m <sup>2</sup> /s	8.22	0.018	0.0036	0.0004	0.0016
	λ <sub>2</sub> , μm	206	115	175	196	192

Remarks: D<sub>i</sub><sup>S</sup> values are given at t = 1500 °C; the values of τ<sub>LS</sub> and λ<sub>2</sub> is shown for axial area.

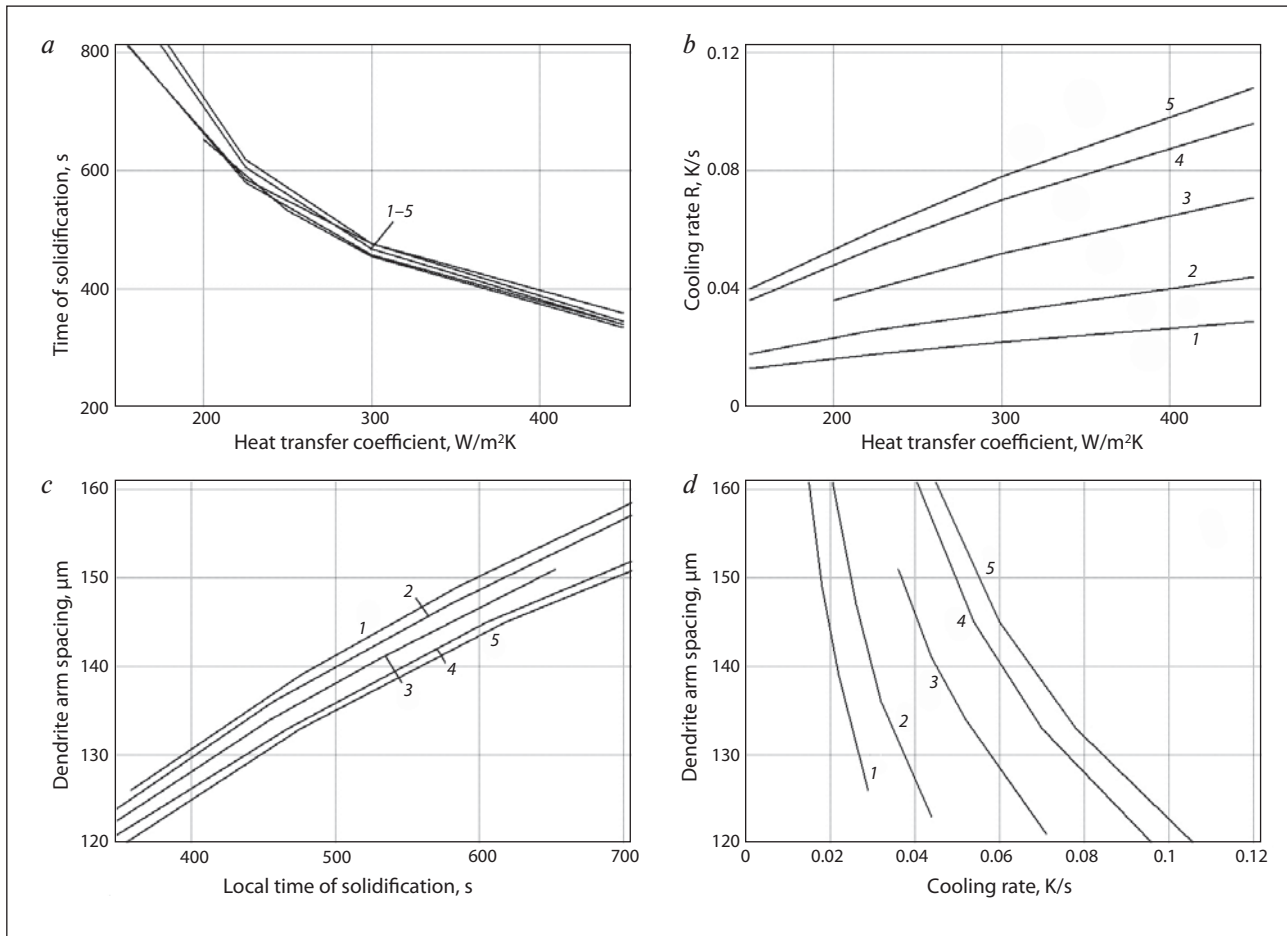


**Fig. 2.** Effect of local solidification time  $\tau_{LS}$  (a) and cooling rate  $R$  (b) on the values of dendrite arm spacing  $\lambda_2$  (c, d) for alloys at different intensity of heat removal and carbon content (in the center of 240 mm thick billets) C, %: 1 – 0.01; 2 – 0.02; 3 – 0.04; 4 – 0.06; 5 – 0.07

( $K_2 = 15.7\text{--}17.3 \mu\text{m/s}^m$ ) and differ a little for different carbon content ( $K_2 = 16.9\text{--}17.8 \mu\text{m/s}^m$ ), being satisfactorily correlated with the experimental data (see table 2 in the part 1).

Statistical models (see table 3), describing the effect of composition of multi-component alloys on their microstructure [14, 17, 20, 38 etc.], in several cases have artificial character and can't be used for interpretation of the obtained data. It is expedient to accept the canonic expression  $\lambda_2 = K\tau_{LS}^m$ , as a rational mathematical construction for presenting empiric and calculated data. This expression reflects adequately the effect of thermal-physical conditions of forming the structure (see formulas (6) and (7)), with proportionality coefficient  $K$ , reflecting the effect of alloy composition via additional concentration multiplier that has analytically simple and physically apprehensible polynomial form (see the formulas (5), (7) and (10) in the table 1):

$$\lambda_2 = K_0(1 + \sum b_i C_i + \sum b_{ij} C_i C_j + \sum b_{ii} C_i^2) \tau_{LS}^m, \quad (8)$$

where regression coefficients of linear ( $b_i$ ) non-complete quadratic ( $b_i, b_{ij}$ ) or quadratic ( $b_i, b_{ij}, b_{ii}$ ) model are calculated via statistical analysis [41] of experimen-

tal data collection including  $\lambda_2/\tau_{LS}^m$  values. The effect of carbon content in out-peritectic alloys at  $C \leq 0.07\%$  (see table 3) is described by the summarized expression (formula (16) in the table 3):

$$\lambda_2 = 18,39(1 - 0,731C) \tau_{LS}^{0,329}, \quad (9)$$

that is based on the data collection with number  $N$  more than 20 points and is characterized by the values of correlation coefficients  $R_1 = 0.989$  (on the stage of logarithmic linearization of  $\lambda_2 = K\tau_{LS}^m$  expression during  $m = 0.329 \pm 0.038$  determination), as well as  $R_2 = 0.984$  (on the stage of  $K_0 = 18.39 \pm 0.02 \mu\text{m/s}^m$  and of  $b_C = 0.73 \pm 0.03 \text{ 1/wt.}\%$  coefficient evaluation, its value is close to the values in the formulas (2), (4), (9) and (12) on the fig. 1).

**Numerical analysis of the effect of steel components on the values of dendritic arm spacing.** Variation of  $\lambda_2$  value during separate introduction of 1% of Si, Mn, Cr or Ni in the melt with carbon content 0.06% and 0.6% is presented in the table 4 and on the fig. 3 for comparative evaluation of influence of separate steel components in forming dendritic structure. Joint effect of the presented thermal-physical and physical-chemical factors leads to

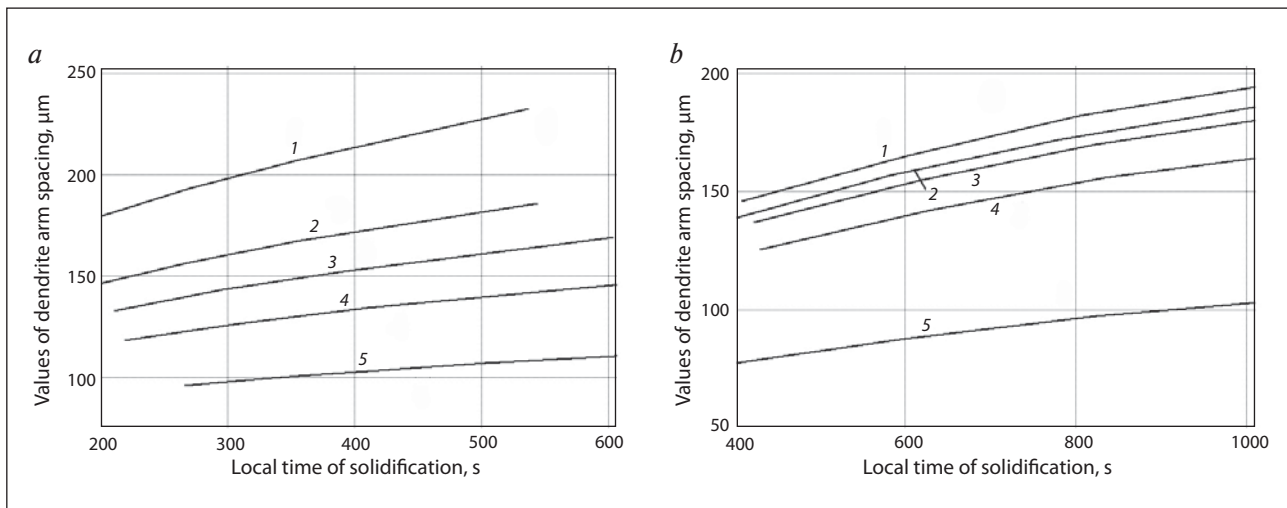


**Fig. 3.** The effect of steel components – C (1), Cr (2), Ni (3), Mn (4) и Si (5) on the values of secondary dendritic arm spacing  $\lambda_2$  in the alloys with carbon content 0.06 (a) и 0.60 (b) %, depending on local time of solidification (in the center of billets with 240 mm thickness)

substantial difference in solidification time of the alloys characterized by different content of components.

However, the features of the effect of components on the values of dendritic arm spacing  $\lambda_2$  are determined not by variation of thermal-physical parameters, but by the complex of physical-chemical factors (as can be concluded from the table 4). The effect of these physical-chemical factors provides forming composition of liquid phase and diffusion redistribution of the components between dendritic arms. Introduction of any of researched components (Si, Mn, Cr and Ni) in the alloy containing carbon results in decrease of  $\lambda_2$  value, while its intensity increases as follows: Cr-Ni-Mn-Si, and causes substantial enlargement of dispersity of dendritic structure.

This consequence is determined by the value of parametrical complex  $p_i(1 - k_i)C_i^L/D_i^L$  (see table 4), located under summation sign in denominator of (6) и (7) formulas. The leading role among these parameters is related to  $k_i$  and  $p_i$ , which determine important role of carbon (in spite of its relatively low concentration) and high specific effect of silicon. Additionally, widening of concentration solidification interval  $\Delta C_i = (1 - k_i)C_i^L$  provides origination and development of heterogeneity of melt composition near inter-phase boundary.

Logarithmic relationships  $\lambda_2(\tau_{LS})$  obtained during statistical analysis for separate components at C = 0.06% are adequately described by the equations  $\lambda_2 = K_2\tau_{LS}^m$  at  $m \approx 0.33-0.34$  and  $K_2$  ( $\mu\text{m}/\text{s}^m$ ) values that are substantially different for different components ( $K_2^C = 42.7$ ;  $K_2^{\text{Si}} = 14.8$ ;  $K_2^{\text{Mn}} = 22.4$ ;  $K_2^{\text{Cr}} = 31.4$ ;  $K_2^{\text{Ni}} = 26.6$ ). Similar regularities are presented on the fig. 3, b for the alloys with carbon content C = 0.6%. Corresponding logarithmic relationships  $\lambda_2(\tau_{LS})$  at C = 0.6% are characterized by lower values of  $K_2$  coefficients ( $K_2^C = 21.5$ ;  $K_2^{\text{Si}} = 12.8$ ;  $K_2^{\text{Mn}} = 18.7$ ;  $K_2^{\text{Cr}} = 20.5$ ;  $K_2^{\text{Ni}} = 20.2$ ).

Table 3 presents resulting relationships (formulas 17–19, see table 1), connecting the values of secondary dendritic arm spacing  $\lambda_2$  with chemical composition of the alloys at fixed ( $R = 0.99$  for equations (17–18)) and variable ( $R = 0.778$  for equation (19)) carbon content. These relationships reflect features of extraction of  $\delta$ - or  $\gamma$ -phase. The a.m. formulas are different in comparison with empiric equations (1–14) in such way, that they reflect independent effect of different steel components, expressed by regression coefficients  $b_i$  with assistance of linear statistical model of (8) type. The equation (15) is obtained on the base of the results of numerical simulation of forming of dendritic structure in the axial area during solidification of 240 mm thick slab made of 10KhGN2 (10XГH2) steel according to the above-described technique [42]. To reveal separate and joint effect of steel components on the values of dendritic arm spacing  $\lambda_2$ , their content was simultaneously varied in multi-component composition (fraction factor experiment  $2^{4-1}$ , generating relationship  $X_4 = X_1X_2X_3$ ) in correspondence with the technique of experiment orthogonal planning [41]. It will provide absence of mutual correlation in content of alloy components during building of multi-factor statistical model.

The exponent for  $\tau_{LS}$  was obtained via logarithmic linearization for more than 30 points in a billet cross section. Presented regression coefficients  $b_i$  and  $b_{ij}$  display that, in addition to the main linear diminishing effect  $\lambda_2$ , during introduction of each of the researched components their mutual effect takes place; it decreases linear effect the more intensively, the larger is content of interacting components. Features of the presented equations (1–19) is concluded in the fact that the values of coefficients reflecting different influence of investigated elements have local character, typical for statistical models, i.e. they correspond to the concrete averaged alloy composition.

\* \* \*

The review of publications on dependence of dendrite arm spacing microstructure of carbon and low-alloy steels from their chemical composition testifies that evaluation of this effect obtained by experiments and presented by statistical models, is characterized by significant differences in mathematical form, as well as the sign and magnitude of the regression coefficients which evaluate the contribution of different components of steel. As a result, the collection of presented models has contradictory character, that does not allow its unambiguous usage for governing of dendrite arm spacing by modification of steel composition and varying the determining factors.

Improvement of the quality of statistical models (the exception of insignificant effects caused by certain components, elimination the correlation distortion, etc.) and ensuring of their adequacy can be achieved via reasonable unification the description of the experimental data on the basis of a polynomial form of the concentration term of the regression equation, obtained by means of orthogonal experimental design.

Computer-aided analysis of forming dendritic structure on the base of calculation of non-equilibrium solidification, taking into account the changes in the composition of the liquid phase and the evolution of dendrite arm spacing, allows quantitative evaluation of the role of physical-chemical and thermal-physical factors in the development of coalescence of secondary arms. It is established the reduction of the secondary dendrite spacing in carbon and low alloy steels with growth of carbon, silicon, manganese, chromium, and nickel content, as well as the increase in the proportion of austenite during solidification, due to the suppression of diffusion transport of components during coalescence of dendritic branches.

V. M. Golod<sup>1</sup>, K. I. Emelyanov<sup>1</sup>, I. G. Orlova<sup>1</sup>

<sup>1</sup> Saint-Petersburg State Polytechnic University  
(St. Petersburg, Russia)

E-mail: cheshire@front.ru

© Golod V. M., Emelyanov K. I., Orlova I. G., 2013

## REFERENCES (Part 2)

36. Golod V. M., Emelyanov K. I., Orlova I. G. Prediction of dendritic micro-heterogeneity of cast steel: review of models and computer-aided analysis of problems. (Part 1. Models based on thermal-physical parameters). — CIS Iron and Steel Review. 2013. pp. 21–28.
37. Taha M. A. Some observations of dendritic morphology and dendrite arm spacing. *Metal Science*. 1979. No. 1. pp. 9–12.
38. Guo W., Zhu M. Characteristic parameters for dendritic microstructure of solidification during slab continuous casting. *Journal of Iron and Steel Research, International*. 2009. Vol. 16, No. 1. pp. 17–21.
39. Han Q., Hu H., Zhong X. Models for the isothermal coarsening of secondary dendrite arms in multicomponent alloys. *Metallurgical and Materials Transactions*. 1997. Vol. 28B, No. 6. pp. 1185–1187.
40. Miettinen J. Thermodynamic-kinetic simulation of constrained dendrite growth in steel. *Metallurgical and Materials Transactions*. 2000. Vol. 31B, No. 2. pp. 365–379.
41. Nalimov V. V., Chernova A. A. *Statisticheskie metody planirovaniya ekstremalnykh eksperimentov* (Statistical methods of design of extremal experiments). Moscow: Nauka, 1965. 340 p.
42. Golod V. M., Emelyanov K. I., Orlova I. G. Dendritnaya mikroneodnorodnost stalnykh otlivok: obzor issledovaniy i kompyuternyy analiz. Sbornik "Liteynoe proizvodstvo segodnya i zavtra". Trudy 9 Vserossiyskoy nauchno-tekhnicheskoy konferentsii (Dendritic microinhomogeneity of steel founding: review of researches and computer analysis. Collection "Foundry today and tomorrow". Proceedings of the 9-th All-Russian scientific and technical conference). Saint Petersburg, Publishing House of Polytechnical University, 2012. pp. 436–455.

## Prediction of dendritic micro-heterogeneity of cast steel: review of models and computer-aided analysis of problems (Part 3. Local structural and chemical heterogeneity)

*In the third part of the review it is noted that the number of publications devoted to the problem of heterogeneity of dendritic structure on the microscale, is very little. They have no significant results and methods that can reveal the basic laws of the evolutionary transformation of secondary dendritic branches from the moment of their inception to the final state. The coalescence models of dendritic*

*branches are traditionally used to calculate the average value of the secondary dendrite spacing. The experimental data evaluates considerable scatter of dendrite arm spacing relative to the average values with a coefficient of variation  $V = 0.20-0.25$ .*

*Using a Monte Carlo simulation, it was implemented the solution of formation of an array of data, according to*